

Realistic rotating convection in a DNA suspension

D. Laroze^{a,*}, J. Martínez-Mardones^b, J. Bragard^c, C. Pérez-García^{c,✉}

^a*Departamento de Física, Facultad de Ciencias Físicas y Matemáticas, Casilla 487-3, Santiago, Chile*

^b*Instituto de Física, Universidad Católica de Valparaíso, Casilla 4059, Valparaíso, Chile*

^c*Departamento de Física y Matemática Aplicada, Universidad de Navarra, E-31080 Pamplona, Spain*

Received 27 December 2005; received in revised form 16 January 2007

Available online 16 May 2007

Abstract

In this work we report theoretical and numerical results on convection in a viscoelastic binary mixture under rotation for realistic rigid–rigid boundary conditions. We focus our analysis in the DNA aqueous suspensions. Instability thresholds for oscillatory convection are calculated. Finally, we analyze the stabilizing effect for the onset of convection.

© 2007 Elsevier B.V. All rights reserved.

Keywords: Thermal convection; Viscoelastic fluid; Binary mixture

1. Introduction

Dilute suspensions of long DNA molecules display viscoelastic properties [1]. Usually, DNA fragments mixed with thermostable polymerase enzyme are heated until the temperature required to unbound the double helix is reached. Then the mixture is annealed, and DNA fragments are doubled by the polymerase enzyme; after several thermal cycles a high concentration of DNA is obtained. This is known as polymerase chain reaction (PCR), a technique usually found in biochemistry laboratories [2]. Thermal cyclers in standard PCR heat and cool not only the whole reaction volume, but also the surrounding vessel and its fitting. This implies a large thermal mass which delays heating and cooling.

Kolodner has reported oscillatory convection in suspensions of DNA in an annular container heated from below; this author comments that the observed properties cannot be explained by a mere viscoelastic model but that composition effects must be taken into account [3]. These results inspired Martínez-Mardones et al. to determine theoretically the convective thresholds in binary viscoelastic mixtures under a vertical temperature gradient [4]. Recently, Braun et al. performed a beautiful experiment in which thermal convection replaces more efficiently the thermal cyclers often used to replicate DNA in the PCR; an essential condition to optimize this thermal process is that convection remains laminar [5]. To improve further this convection PCR technique it would be desirable to explore in detail the different regimes of convection in DNA suspensions.

*Corresponding author.

E-mail address: david.laroze@gmail.cl (D. Laroze).

✉Deceased.

On the other hand, it is well known that centrifugation may alter DNA replication. Moreover, the rotation is another effect that can modify convection. In general, rotation has a stabilizing effect on convection [6]. Rotating convection in Newtonian fluid [7], binary mixture [8], and viscoelastic fluids [9] have been extensively studied. Hence, motivated by the experiments in DNA centrifugation and PCR convection we analyzed, in a previous paper, the role of rotation on thermal convection of a binary viscoelastic fluid for idealized free–free boundary conditions [10].

In the present work, we report theoretical and numerical results on convection in suspensions of DNA under rotation for realistic rigid–rigid boundary conditions. The linear stability analysis of the conduction state is studied in the framework of Navier–Stokes equations for binary mixtures whose viscoelastic properties are described through Oldroyd type constitutive equation, in the Boussinesq approximation. The paper is organized as follows: In Section 2, the basic hydrodynamic equations for binary viscoelastic convection are presented. In Section 3, the linear stability analysis of the conduction state is performed, and the conditions for the onset of convection are discussed. Finally, conclusions are presented in Section 4.

2. Basic equations and boundary conditions

Fig. 1 gives a schematic description of the setup geometry. We consider a layer of incompressible binary viscoelastic fluid, of thickness d and very large horizontal extension, in a gravitational field and submitted to a vertical temperature gradient. The layer is rotating uniformly about the vertical direction with uniform angular velocity ϖ . Let us choose the z -axis such that $\mathbf{g} = -g\hat{\mathbf{z}}$ and that the layer has its interfaces at $z = 0$ and $z = d$. A static temperature difference across the layer is imposed, $T(z = 0) = T_0 + \Delta T$ and $T(z = d) = T_0$. The top and bottom walls are assumed to be conducting and impermeable, so that the polymeric concentration satisfies $\partial_z(N + (k_T/T_0)T) = 0$ at both interfaces, where k_T is the Soret coefficient. Under the Boussinesq approximation, the dimensionless balance and constitutive perturbation equations of the conduction states read as [10]

$$\nabla \cdot \mathbf{v} = \mathbf{0}, \quad (1)$$

$$P^{-1}(\partial_t + \mathbf{v} \cdot \nabla)\mathbf{v} = -\nabla p + \nabla \cdot \boldsymbol{\tau} + ((1 + \psi)\theta + \psi\eta)\hat{\mathbf{z}} + T_a^{1/2}\mathbf{v} \times \hat{\mathbf{z}}, \quad (2)$$

$$(\partial_t + \mathbf{v} \cdot \nabla)\theta = Ra_w + \nabla^2\theta, \quad (3)$$

$$(\partial_t + \mathbf{v} \cdot \nabla)(\eta + \theta) = Ra_w + L\nabla^2\eta, \quad (4)$$

$$(1 + \Gamma D_t)\boldsymbol{\tau} = (1 + \Lambda \Gamma D_t)\mathbf{D}, \quad (5)$$

where $\mathbf{v} = (u, v, w)^T$ is the velocity field, $\boldsymbol{\tau}$ extra stress tensor, θ the temperature, and p the pressure. The auxiliary variable η is simply defined as $\eta = c - \theta$, where c is the dimensionless polymer concentration. Also the following groups of dimensionless numbers have been introduced: (a) (pure fluids) the Rayleigh number $Ra = \alpha g \Delta T d^3 / \kappa \nu$ accounting for buoyancy effects and the Prandtl number $P = \nu / \kappa$, relating viscous and thermal dissipations; (b) (rotation in pure fluids) the Taylor number $T_a = (2\varpi d^2 / \nu)^2$, (c) (binary mixtures) the

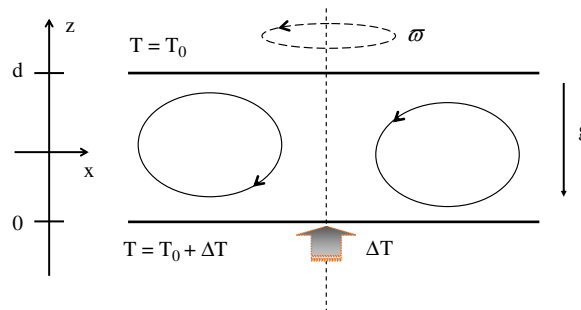


Fig. 1. A vertical cut through the fluid layer. Note the y -axis point into the xz -plane.

Lewis number $L = D/\kappa$, relating diffusion with thermal diffusivity, and the separation ratio $\psi = \beta k_T/\alpha T_0$, and (d) (viscoelasticity) the Deborah number $\Gamma = \lambda_1 \kappa/d^2$ and the ratio between retardation and stress relaxation times $A = \lambda_2/\lambda_1$. In addition, the symbol D_t in Eq. (5) denotes an invariant (frame-indifferent) time derivative, defined as $D_t \boldsymbol{\tau} = (\partial_t + \mathbf{v} \cdot \nabla) \boldsymbol{\tau} + \boldsymbol{\tau} \cdot \mathbf{W} - \mathbf{W} \cdot \boldsymbol{\tau} + a(\boldsymbol{\tau} \cdot \mathbf{D} + \mathbf{D} \cdot \boldsymbol{\tau})$, where \mathbf{W} and \mathbf{D} are the skew-symmetric and symmetric parts of the velocity field gradient, respectively; also a is a phenomenological parameter in the range -1 to $+1$. To solve this system of equations, the realistic rigid–rigid boundary conditions for velocity: $w = \partial_z w = \partial_z \eta = \theta = 0$, at both $z = 0$ and $z = 1$ are imposed. In the next section, we study the corresponding linear stability analysis of the conduction state.

3. Linear stability analysis and results

For calculating the linear stability analysis, we only need the linear parts of Eqs. (1)–(5); it is easily obtained by neglecting nonlinear terms containing $(\mathbf{v} \cdot \nabla)$ and replacing D_t by ∂_t . The pressure term is eliminated after applying the curl operator twice to the linear momentum equation. These operations produce a set of equations in matrix form

$$\mathbf{L} \cdot \mathbf{X} = \mathbf{0}, \tag{6}$$

where $\mathbf{X} = \mathbf{X}(\mathbf{r}, t)$ is defined by $\mathbf{X} = (\theta, \phi, w, \zeta)^T$ and ζ denotes the z -component of the vorticity. The linear differential operator \mathbf{L} is defined as

$$\begin{pmatrix} \partial_t - \nabla^2 & 0 & 0 & -R_a \\ \partial_t & \partial_t - L\nabla^2 & 0 & -R_a \\ 0 & 0 & P^{-1}\partial_t \Pi_t - \Xi_t \nabla^2 & T_a^{1/2} \Pi_t \partial_z \\ -(1 + \psi) \Pi_t \nabla_{\perp}^2 & -\psi \Pi_t \nabla_{\perp}^2 & -T_a^{1/2} \Pi_t \partial_z & P^{-1} \partial_t \Pi_t \nabla^2 - \Xi_t \nabla^4 \end{pmatrix}, \tag{7}$$

where $\nabla^2 = \partial_x^2 + \partial_y^2 + \partial_z^2$, $\nabla_{\perp}^2 = \partial_x^2 + \partial_y^2$, $\Pi_t = 1 + \Gamma \partial_t$, and $\Xi_t = 1 + A\Gamma \partial_t$. For the realistic boundary conditions, the space-temporal dependencies of $\mathbf{X}(\mathbf{r}, t)$ are separated by the usual normal mode expansion:

$$\mathbf{X}(\mathbf{r}, t) = (\Theta, \Phi, W, Z)(z) \exp[i\mathbf{k} \cdot \mathbf{r}_{\perp} + st], \tag{8}$$

where \mathbf{k} the horizontal wavenumber vector and where $s = \sigma + i\Omega$ denote the complex eigenvalues; σ is the growth factor of a perturbation and Ω its frequency. This leads to the following coupled ordinary differential equations:

$$\Theta^{II} = (s + k^2)\Theta - R_a W, \tag{9}$$

$$L\Psi^{II} = (s + Lk^2)\Psi + s\Theta - R_a W, \tag{10}$$

$$PQZ^{II} = (s + PQk^2)Z - PT_a^{1/2} W^I, \tag{11}$$

$$W^{IV} = (2k^2 + s/PQ)W^{II} + (T_a^{1/2}/Q)Z^I + (k^2/Q)[\psi\Phi + (1 + \psi)\Theta - (Qk^2 + s/P)W], \tag{12}$$

where $Q = (1 + \Gamma As)/(1 + \Gamma s)$ and $f^I = \partial_z$, $f^{II} = \partial_z^2$, etc. In order to solve the set of differential equations (9)–(12) we use a spectral method. We have followed the technique of collocation points in a Chebyshev grid described by Trefethen [11]. We have chosen 14 collocation points in the vertical direction. This converts the differential equations plus the boundary conditions into a generalized eigenproblem with the eigenvectors being the discretized eigenfunctions $(\Theta(z), \Phi(z), W(z), Z(z))$ and the corresponding eigenvalues provided a set of Rayleigh numbers. Since the physical Rayleigh numbers are real but the eigenvalues are in general complex, we have to iterate by using different values of the frequency in order to get a vanishing imaginary part of the eigenvalues to obtain the corresponding Rayleigh number R_a . This gives a triplet of point (R_a, k, Ω) for each given parameter value. We repeat this procedure for several values of the horizontal wavenumber which permits to draw a curve of the real part of the Rayleigh number as a function of this wavenumber. The minimum of this curve determines the critical values R_{ac} and k_c , and also the associated critical frequency Ω_c .

Let us discuss a little more about the physical meaning of the different parameters. First, concerning the viscoelastic parameters, the Deborah number, Γ , corresponds to the measure of the fluid memory effect; and the ratio between retardation and stress relaxation times, A , corresponds to the measure of the timescale of the

memory effect. The parameters related to the mixture of the binary fluid are, the Lewis number, L , that controls the relaxation between the thermal and mass diffusion; and the separation ratio, ψ , measuring the Soret effect. It comes from the analysis that the parameters R_a and T_a may span a range of several orders of magnitude while Γ , which relates a typical relaxation time to the thermal diffusion time, usually changes by only one order of magnitude. The remaining parameters P , A , L , and ψ depend only on the properties of the fluid. A typical value for P is $P \approx 10$ (water). For $A = 1$ one recovers a Newtonian fluid while for $A = 0$ a Maxwellian fluid is described. For aqueous suspensions of DNA L ranges between 10^{-5} and 10^{-4} [2] and results in Ref. [12] suggest that the Deborah number could vary in the range $\Gamma = 0.1–1.2$. Unfortunately, no experimental data are available neither for the separation ratio ψ nor for the retardation time A , so we have used a slightly negative value of ψ and several values of A .

The main results are displayed in Figs. 2 and 3, where we plot the critical Rayleigh number R_{ac} and the critical frequency Ω_c as function of the Deborah number Γ for $L = 10^{-4}$, $\psi = -10^{-4}$ and $A = (0, 0.75, 1)$; two different Taylor number values are considered: $T_a = 10$ (Fig. 2) and $T_a = 10^3$ (Fig. 3), respectively. For the lower value of rotation, $T_a = 10$, when $A = 1$ (Newtonian fluid) the critical values R_{ac} (Fig. 2a) and Ω_c (Fig. 2b) remain nearly constant and with relatively low values. Whereas both critical values are very high for a purely Maxwell fluid ($A = 0$), but they decrease when Γ is increased. For the intermediate value $A = 0.75$, the critical values first increase for low values of Γ , and then they slightly decrease when Γ is further increased.

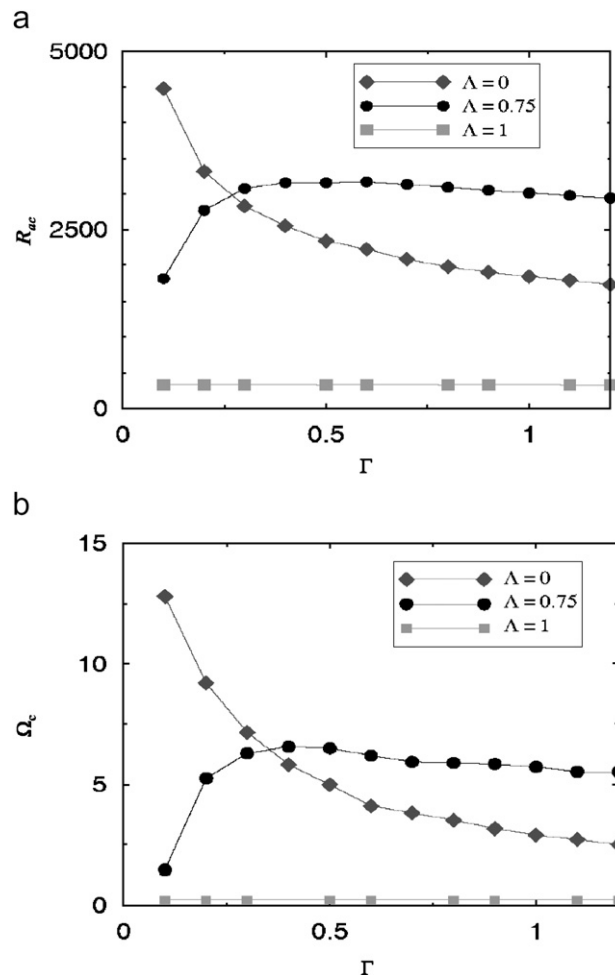


Fig. 2. (a) Critical Rayleigh number R_{ac} and (b) critical frequency Ω_c for oscillatory instability as function of the Deborah number Γ for a low rotation rate $T_a = 10$.

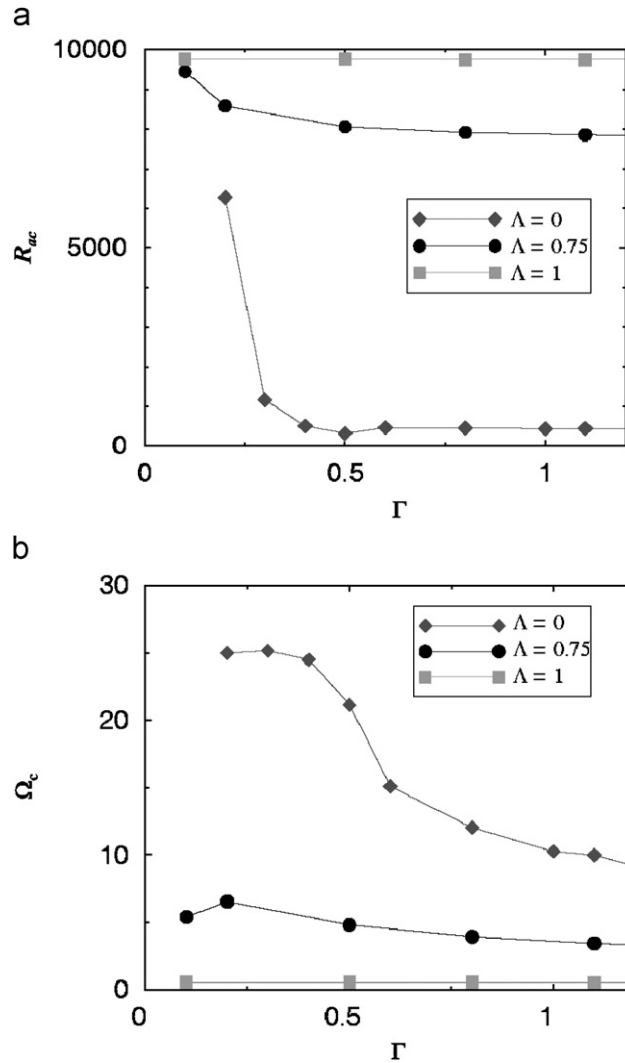


Fig. 3. (a) Critical Rayleigh number R_{ac} and (b) critical frequency Ω_c for oscillatory instability as function of the Deborah number Γ for a high rotation rate $T_a = 10^3$.

The case of a high rotation rate, $T_a = 10^3$, is shown in Fig. 3. The curves show that rotation stabilizes a Newtonian fluid [6], but it destabilizes a Maxwellian fluid [9]. For intermediate values of Λ ($\Lambda = 0.75$), viscoelastic properties couple with rotation to lower the convective threshold R_{ac} and rise the critical frequency Ω_c with respect to the values for a Newtonian fluid. Therefore, in the case of Maxwellian and Newtonian fluids the effect of rotation is opposite, destabilizing and stabilizing, respectively.

Let us comment about some differences related to the choice of boundary conditions i.e. free–free or rigid–rigid. In a previous work [10], the case of idealized boundary conditions (free–free) has been analyzed and it has been found that, for the Maxwellian viscoelastic fluid, two distinct regimes were observed [10]. For the critical Rayleigh number and the critical frequency: small values of Γ lead to small critical frequencies regardless of rotational effect; for intermediate values of Γ , Ω_c jumps to a finite value that decreases further increasing Γ . Moreover, the value for which Ω_c jumps increases with T_a ; also we recall that this transition feature appears also for non-rotating system [4]. In contrast, in the present analysis where rigid–rigid boundary conditions are considered there is no such transition neither for non-rotating [4] nor for rotating convection; furthermore, we observe that for Maxwellian viscoelastic fluid R_{ac} is a decreasing function of Γ irrespective of the rotation rate.

4. Conclusions

In the present work we have analyzed the instability thresholds in suspensions of DNA under rotation for realistic rigid–rigid boundary conditions. We have shown that viscoelastic properties stabilize convection under a small rotation rate; on the contrary, they may produce a destabilizing effect for sufficiently high rotation rates, although rotation stabilizes convection in Newtonian fluid. These results suggest that rotation can be used as a tool to enhance the range of the laminar regime of convective cycles to replicate DNA in aqueous solutions.

Acknowledgments

This research received financial support from MECESUP USA-0108, MECESUP FSM-0204, the Millennium Science Initiative from Chile, Grant Anillo ACT 15 and ACT 24 of Bicentennial Program of Sciences and Technology-Chile and the DGICYT (Spanish Government) under Grant BFM 2002-02011. J.B. acknowledges financial support from MEC project (Spain) FIS2005-06912-C02 (DINCARD).

References

- [1] T.T. Perkins, D.E. Smith, S. Chu, *Science* 264 (1994) 822.
- [2] G.J. Nuovo, *PCR in situ Hybridization: Protocols and Applications*, Lippincott-Raven, Philadelphia, 1997.
- [3] P. Kolodner, *J. Non-Newtonian Fluid Mech* 75 (1998) 167.
- [4] J. Martínez-Mardones, R. Tiemann, D. Walgraef, *Physica A* 283 (2000) 233.
- [5] D. Braun, N.L. Goddard, A. Libchaber, *Phys. Rev. Lett.* 91 (2003) 158103.
- [6] S. Chandrasekhar, *Hydrodynamics and Hydromagnetic Stability*, Oxford University Press, Oxford, 1961.
- [7] J.K. Bhattacharjee, *Phys. Rev. A* 37 (1988) 1368.
- [8] E. Bodenschatz, G. Ahlers, W. Pesch, *Ann. Rev. Fluid Mech.* 32 (2000) 709.
- [9] P.K. Bhatia, J.M. Steiner, *ZAMM* 52 (1972) 321.
- [10] D. Laroze, J. Martínez-Mardones, C. Pérez-García, *Int. J. Bifur. Chaos* 15 (2005) 3329.
- [11] L.N. Trefethen, *Spectral Methods in Matlab* SIAM, Philadelphia, PA, 2000.
- [12] D.E. Smith, H.P. Babcock, S. Chu, *Science* 283 (1999) 1724.